RSC Advances

PAPER

View Article Online
View Journal | View Issue

Cite this: *RSC Adv.*, 2014, **4**, 1918

Synthesis of triazole linked fluorescent amino acid and carbohydrate bio-conjugates: a highly sensitive and skeleton selective multi-responsive chemosensor for Cu(II) and Pb(II)/Hg(II) ions†

Arunabha Thakur, Dipendu Mandal, Pranab Deb, Bijan Mondal and Sundargopal Ghosh*

Received 8th August 2013
Accepted 13th November 2013

DOI: 10.1039/c3ra44263b

www.rsc.org/advances

A set of triazole-based chromogenic and fluorescent chemosensors with amino acid/carbohydrate–fluorophore conjugates have been designed and synthesized. The metal cation-sensing properties of glycine–anthracene, $C_{24}H_{24}O_4N_4$ (**3**), glycine–pyrene $C_{26}H_{24}O_4N_4$ (**4**), glucose–anthracene, $C_{32}H_{33}O_{10}N_3$ (**5**) and glucose–pyrene, $C_{34}H_{33}O_{10}N_3$ (**6**) bio-conjugates have been studied systematically. The significant changes in their absorption spectra are accompanied by a strong color change from light yellow to brown for **3** and **4** and colorless to greenish blue for **5** and **6**. Receptors **3** and **4** have potential in the "naked eye" detection of Cu^{2+} and **5** and **6** for Pb^{2+}/Hg^{2+} ion. The receptors **3** and **4** show fluorescence diminution following Cu^{2+} coordination within the limit of detection at 0.89 parts per billion (ppb) and this is unprecedented, whereas the receptors **5** and **6** present drastic fluorescence quenching upon addition of Hg^{2+} and Pb^{2+} within the limit of detection at 4 and 2 ppb respectively. Interestingly, their fluorescence and colorimetric responses are preserved in the presence of water that can be used for the selective colorimetric detection of these ions in aqueous environments. Along with the spectroscopic data, combined ^{1}H NMR titration of the complexes and the DFT studies suggest the proposed coordination modes.

Introduction

Sensing technology and sensors have advanced in the past few decades,[1–4] where chemists play an important role in the progress of chemical sensors. The development of artificial receptors for sensing and the recognition of environmentally and biologically important ionic species, especially transition-metal ions, is currently of great interest.[1–4] A chemical sensor is composed of two structural subunits; a receptor and a signaling unit.[5–12] The signaling unit can give either electrochemical or optical responses. The most popular optical signaling units used by chemists are fluorophore units.[13–17] The two components are intramolecularly connected together such that the binding of the target metal ion causes significant changes to the photophysical properties of the fluorophores, for example, emission intensity, wavelength, or lifetime of the excited state. The signaling and sensory units of a sensor can thus be fabricated in a suitable way so that selectivity towards metal ions can be tuned.

Among the heavy and soft metal cations, mercury is considered as the most prevalent toxic metal and has severe effects on human health and the environment because of its wide distribution and severe immunotoxic, genotoxic, and neurotoxic effects.[18,19] The accumulation of lead in the body can result in neurological, reproductive, cardiovascular and developmental disorders.[20] On the other hand, copper is the third most abundant heavy metal (after Fe^{3+} and Zn^{2+}) in human body and is very essential as a catalytic co-factor in metalloenzymes like superoxide dismutase, cytochrome *c* oxidase or tyrosinase. Further excess copper cause neurodegenerative diseases, like Alzheimer's and Wilson's disease and is also suspected to cause amyloidal precipitation and toxicity.[21–26] As a result, the development of new methods for the sensitive and selective detection of these heavy metals are highly desirable. Keeping these backgrounds, a variety of methods have been developed to monitor the toxic metal cations contamination in water, food, soil, and so on. Among the various methods to monitor toxic metal ions under the toxicological and environmental conditions, fluorescence chemosensors are widely regarded as one of the most effective methods. Although great efforts have been

Department of Chemistry, Indian Institute of Technology Madras, Chennai, 600 036, India. E-mail: sghosh@iitm.ac.in; Fax: +91 44-22574202; Tel: +91 44-22574230

† Electronic supplementary information (ESI) available ^{1}H, ^{13}C and ESI-MS data of **3–6**; UV-vis spectra upon titration with different metal ions of **3**; ESI-MS spectrum of [**3**·Cu^{2+}], [**4**·Cu^{2+}], [**5**·Pb^{2+}], [**5**·Hg^{2+}], [**6**·Pb^{2+}], [**6**·Hg^{2+}]; The quantitative binding data for **3** and **4** with Cu^{2+} and, **5** and **6** with Hg^{2+} and Pb^{2+}, optimized geometry of ligands **4** and **6** and their complexes with the metal corresponding metal ions species. See DOi: 10.1039/c3ra44263b

made to develop several chemosensors for the detection of toxic metal ion,[27–53] the design and advancement of new and practical chemosensors, that offer a promising advance for Cu^{2+} and Pb^{2+} or Hg^{2+} ion, with low limit of detection in aqueous media, is still a great challenge. In this article, we demonstrate the host–guest complexation properties of glycine and carbohydrate based colorimetric chemosensors for Cu^{2+} and Hg^{2+}/Pb^{2+} ion respectively through optical and ^1H NMR titration along with DFT calculations.

Results and discussion

As shown in Scheme 1a, glycine azide undergoes the "click reaction" with anthracene alkyne **1** to generate yellow **3** and with pyrene alkyne **2** to generate yellow **4** in 78% and 81% yield respectively. In a similar fashion, glycosyl azide undergoes "click reaction" with **1** to yield **5** and with **2** it produces yellow **6** in 80% and 84% yield respectively (Scheme 1b). All the compounds have been characterized by ESI-MS, ^1H and ^{13}C NMR spectroscopy and elemental analysis. The metal cation sensing properties of the receptors **3–6** have been investigated by UV-vis and fluorescence spectroscopy and ^1H NMR titration measurements as well as by DFT studies.

UV-visible absorption studies

The UV-vis binding interaction studies of receptors **3–6** were performed in (CH_3CN/H_2O, 2/8) (1×10^{-5} M) against cations of environmental relevance, such as Li^+, Na^+, K^+, Ag^+, Ca^{2+}, Mg^{2+}, Cr^{2+}, Zn^{2+}, Co^{2+}, Fe^{2+}, Tl^+, Hg^{2+}, Cd^{2+} and Pb^{2+} as perchlorate salts. Compounds **3** and **4** show selective response to Cu^{2+}, whereas **5** and **6** show high selectivity towards Pb^{2+} and Hg^{2+}. The change in the UV-vis absorbance spectra of receptors **3** and **4** in (CH_3CN/H_2O, 2/8) due to the stepwise addition of Cu^{2+} ion are shown in Fig. 1. Upon gradual addition of 1 equiv. of Cu^{2+} to **3**, one strong high-energy (HE) absorption band at λ 242 nm (2782 M^{-1} cm^{-1}) along with one typical absorption band centered at 363 nm for anthracene moiety decreased with a concomitant increment of one high energy band at 214 nm (2212 M^{-1} cm^{-1}). In addition, well-defined isosbestic points were observed at 225 nm and 265 nm for **3** indicating the presence of one distinct complex. Addition of 1 equiv. of Cu^{2+} to **4**, the typical absorption band for pyrene moiety red-shifted by 5–6 nm with concomitant increment of one high energy band at 215 nm. The binding assays using the method of continuous variations (Job's plot) strongly suggest 1 : 1 (cation/receptor) complex formation with Cu^{2+} ion for compound **3** and **4** (Fig. 1,

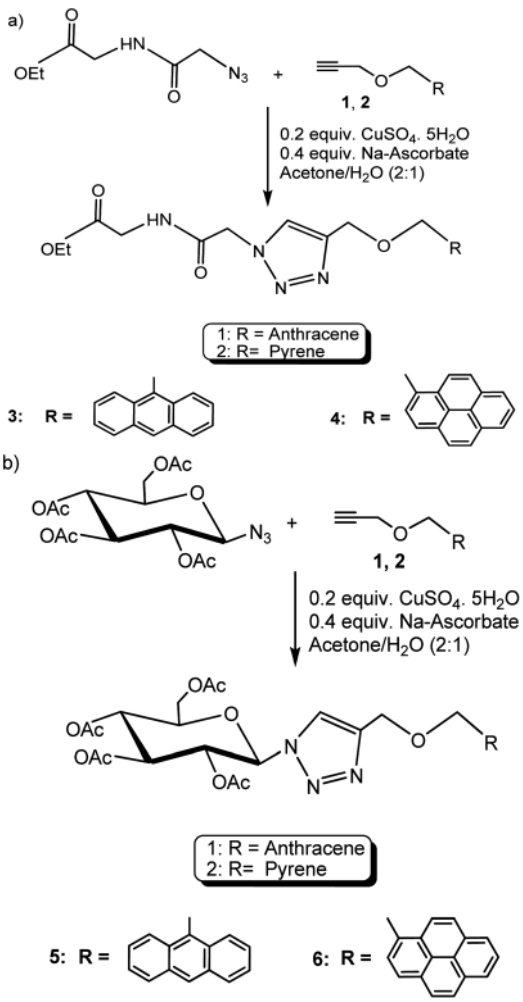

Scheme 1 Synthesis of compounds **3**, **4** (a) and **5**, **6** (b) using "Click reaction".

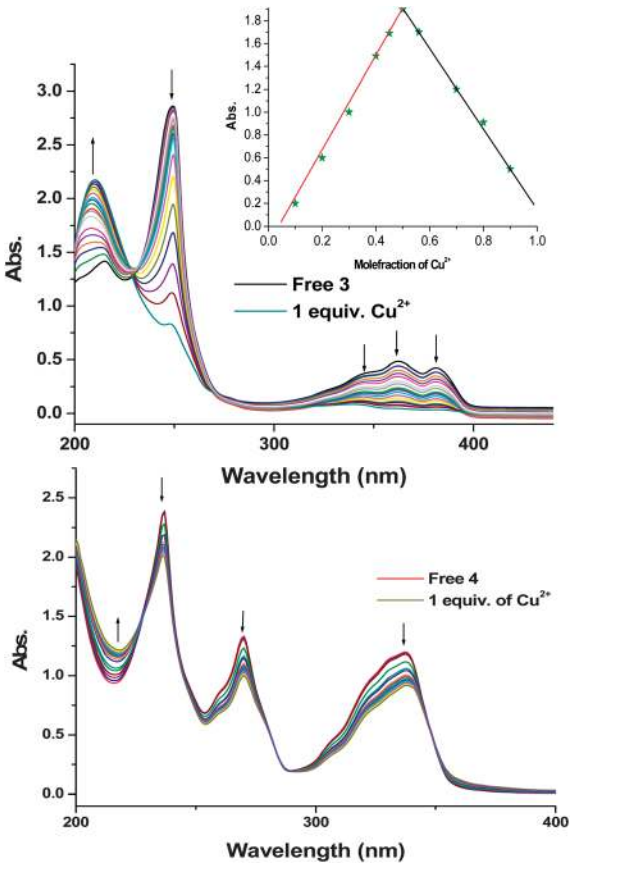

Fig. 1 UV-vis absorbance spectra of **3** (top) and **4** (bottom) (10^{-5} M) upon addition of Cu^{2+} ion up to 1 equiv. in CH_3CN/H_2O (2/8).

inset and ESI, Fig. S1†). Further, the stoichiometry of the complex has also been confirmed by ESI-MS, where peaks at *m*/*z* 495 for [**3**·Cu^{2+}] and *m*/*z* 520 for [**4**·Cu^{2+}] are observed (ESI, Fig. S2 and S3†). The binding constant determined[54] from the increasing absorption intensity at 214 and 215 nm for **3** and **4** is K (±15%) = 4.03×10^6 and 3.82×10^5 M^{-1} respectively.

Likewise, as shown in the Fig. 2, addition of an increasing amount of Pb^{2+} ion to a solution of **5**, one characteristic absorption band centered at 363 nm for anthracene moiety along with one strong high-energy (HE) absorption band at λ 250 nm (2662 M^{-1} cm^{-1}) decreased with a concomitant increment of one high energy band at 206 nm (2658 M^{-1} cm^{-1}). In addition, two well-defined isosbestic points were observed at 219 nm and 262 nm for **5** indicating the presence of unique complex at the equilibrium. Upon addition of 1 equiv. of Pb^{2+} ion to **6**, the HE band at 215 nm (1232 M^{-1} cm^{-1}) increases and red shifted by 6 nm, whereas upon addition of Hg^{2+} ion to **6**, one new energy absorption bands at 252 nm (1564 M^{-1} cm^{-1}) appeared with reduction of other absorption bands characteristic of pyrene subunit. The binding assays using the method of continuous variations (Job's plot) suggest 1 : 1 (cation/receptor) complex formation with Pb^{2+} and Hg^{2+} ion for compounds **5** and **6** (Fig. 3). Further, the stoichiometry of the complexes has been confirmed by ESI-MS, where peaks at *m*/*z* 826 for [**5**·Pb^{2+}], *m*/*z* 819 for [**5**·Hg^{2+}], *m*/*z* 850 for [**6**·Pb^{2+}] and *m*/*z* 843 for [**6**·Hg^{2+}] are observed (ESI, Fig. S4–S7†). The binding constant determined from the increasing absorption intensity for **5** is K (±15%) = 4.3×10^5 for and 4.8×10^5 M^{-1} for Pb^{2+} and Hg^{2+} respectively and for **6**, K (±15%) = 3.35×10^5 and 2.4×10^5 M^{-1} for Pb^{2+} and Hg^{2+} respectively.

Fluorescence studies

The extent to which the fluorescence intensity of receptors **3–6** were affected in presence of selected cations was tested by fluorescence spectroscopy. All the receptors exhibit a strong fluorescence in (CH_3CN/H_2O, 2/8) solution ($c = 1.5 \times 10^{-10}$ M) when excited at λ_{exc} = 363 nm for **3** and **5** and at λ_{exc} = 341 nm for **4** and **6**. The emission spectra of receptors **3** and **5** display typical emission bands at 394, 413 and 436 nm, attributed to anthracene monomeric emission. When Cu^{2+} ion was added to a solution of **3** and **4**, fluorescence was quenched completely. Thus to determine the amount of Cu^{2+} ion required to induce the complete quenching of fluorescence of **3** and **4**, titration experiments were carried out (Fig. 4). After addition of 1 equiv. of Cu^{2+}, the emission of **3** and **4** was completely quenched, indicating the binding of Cu^{2+} ion with the receptors **3** and **4** forming the **3**/Cu^{2+} and **4**/Cu^{2+} complexes. The mole ratio method was applied to examine the stoichiometry of the **3**/Cu^{2+} and **4**/Cu^{2+} complexs,[55] indicating a 1 : 1 stoichiometry. No

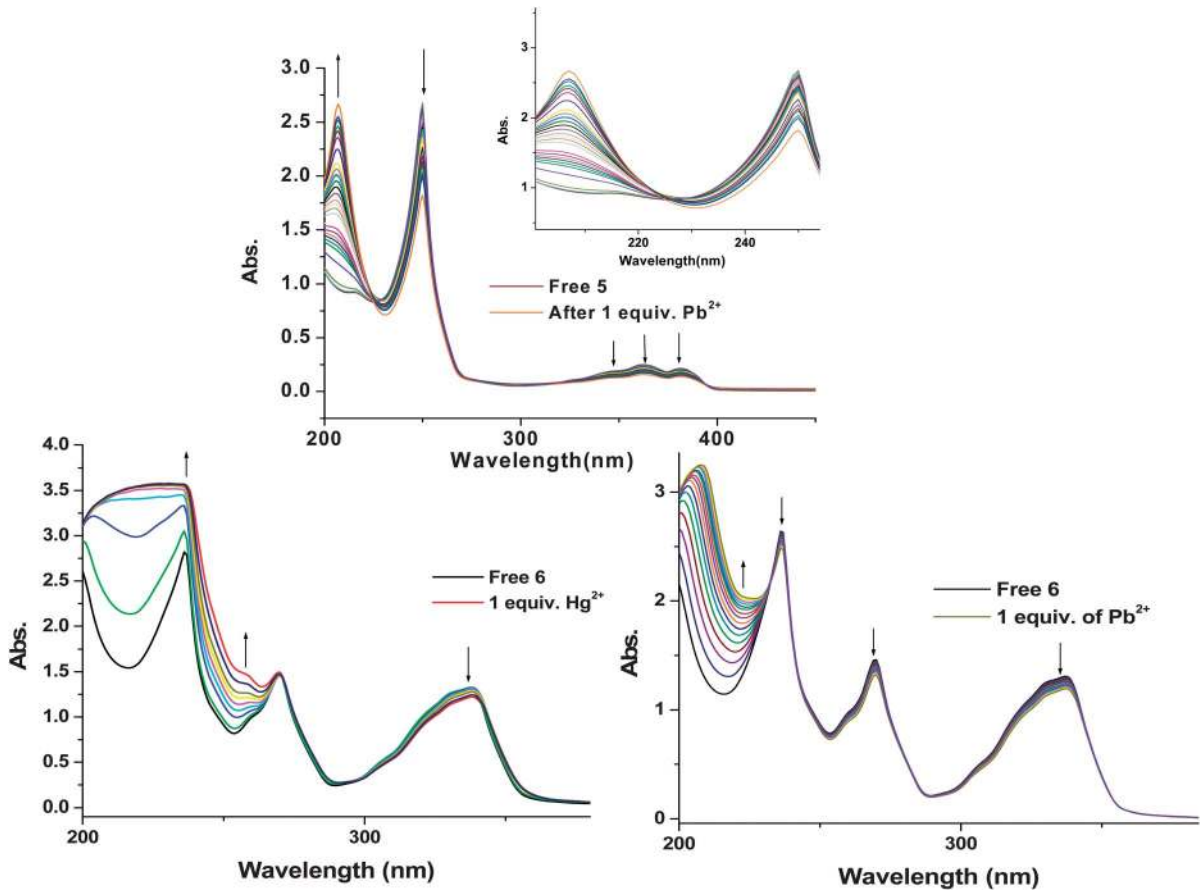

Fig. 2 UV-vis absorbance spectra of **5** (10^{-5} M) (top) upon addition of 1 equiv. of Pb^{2+} ion and **6** (10^{-5} M) (bottom) upon addition of 1 equiv. of Hg^{2+} (left) ion and Pb^{2+} (right) ion in CH_3CN/H_2O (2/8).

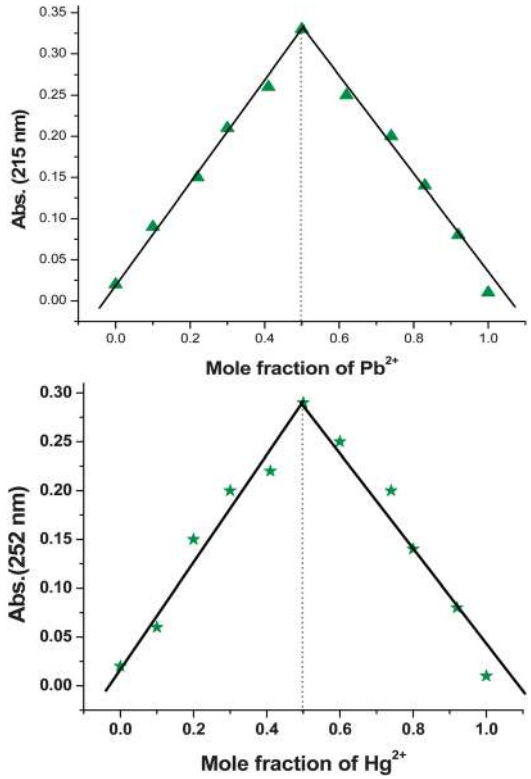

Fig. 3 Job's plot of **6** with Pb^{2+} (top) and with Hg^{2+} (bottom) in CH_3CN indicating the formation of 1 : 1 complex species.

effect of Cu^{2+} ion towards the receptors **5** and **6** was observed whereas, upon addition of 1 equiv. of Pb^{2+} and Hg^{2+} ion the emission band significantly quenched (Fig. 5) may be due to spin–orbit coupling[56] and energy transfer mechanism.[57] Note that the fluorescent behaviour of receptors **3–6** did not undergo any considerable changes upon addition of other metal cations.

To address the sensitivity of the receptors **3** and **4**, we have carried out fluorescence titration of **3** (1.5×10^{-10} M) and **4** (1.5×10^{-10} M) in CH_3CN/H_2O (2/8) with Cu^{2+} ion (1×10^{-6} M) (Fig. 4). The decrease in fluorescence intensity produced by increasing the concentration of Cu from zero to 6 nM is clearly resolved and it has a good signal to-noise ratio. The intensity data were normalized between the minimum intensity (zero free Cu) and the maximum intensity (6.5×10^{-8} M free Cu). A linear curve was fitted to the five intermediate values and the point at which the line crossed the ordinate axis was taken as the detection limit[58] and equaled approximately 0.89 nM (ESI Fig. S8†). In a similar fashion, we carried out the fluorescence titration of **5** (1.5×10^{-10} M) and **6** (1.5×10^{-10} M) in CH_3CN/H_2O (2/8) with Hg^{2+} and Pb^{2+} ion (1×10^{-6} M) (Fig. 6) to ascertain the sensitivity of the receptors towards Hg^{2+} and Pb^{2+} ion. However no such detectable change observed in the fluorescence spectra up to the analyte concentration of 0.15 equiv. for Hg^{2+} and 0.08 equiv. for Pb^{2+}. An appreciable diminution of quantum yield by a factor of 4 is observed in the presence of 0.2 equiv. of Hg^{2+} and 0.1 equiv. of Pb^{2+}, whereas minimum fluorescence intensity was observed in the presence of 1 equiv. of Hg^{2+} or Pb^{2+} for compounds **5** and **6**. The experiment, as performed for Cu^{2+} ion, shows low detectable limit (DL) of Hg^{2+} and Pb^{2+} with **5** or **6**, 4×10^{-9} M (4 ppb) and 2×10^{-9} M (2 ppb) respectively, which are well below the maximum contamination level defined by EPA[59] and a very few chemosensors are reported in the literature which can detect Hg^{2+} and Pb^{2+} ion within this low limit of detection range.[47,60–64] Under optimized condition of 0.1×10^{-10} M and 1.0×10^{-10} M **6** (or **5**) in an aqueous solution (CH_3CN/H_2O, 2/8), two river water samples were analyzed by the proposed fluorimetric method. The fluorescence of **5** or **6** present evident fluorescence quenching in presence of river water samples. The binding constant values of **3–6** with metal ion (Cu^{2+}, Hg^{2+} and Pb^{2+}) have also been determined from the emission intensity data following the modified Benesi–Hildebrand equation[65,66] and it is found that they are in the same order as obtained from UV-vis data.

Further, to evaluate the practical importance of **3** and **4** as a Cu^{2+} selective fluorescence probe, competition experiments were carried out. As a result, a solution of **3** or **4** (1.5×10^{-9} M)

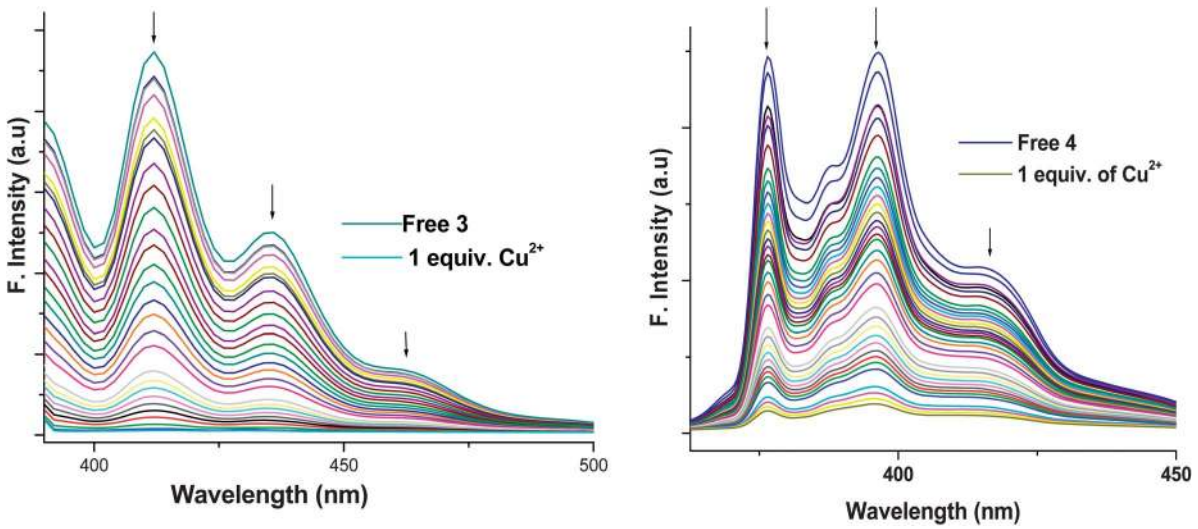

Fig. 4 Fluorescence emission change of **3** (1.5×10^{-10} M) (left) and **4** (1.5×10^{-10} M) (right) upon addition of Cu^{2+} ion upto 1 equiv.

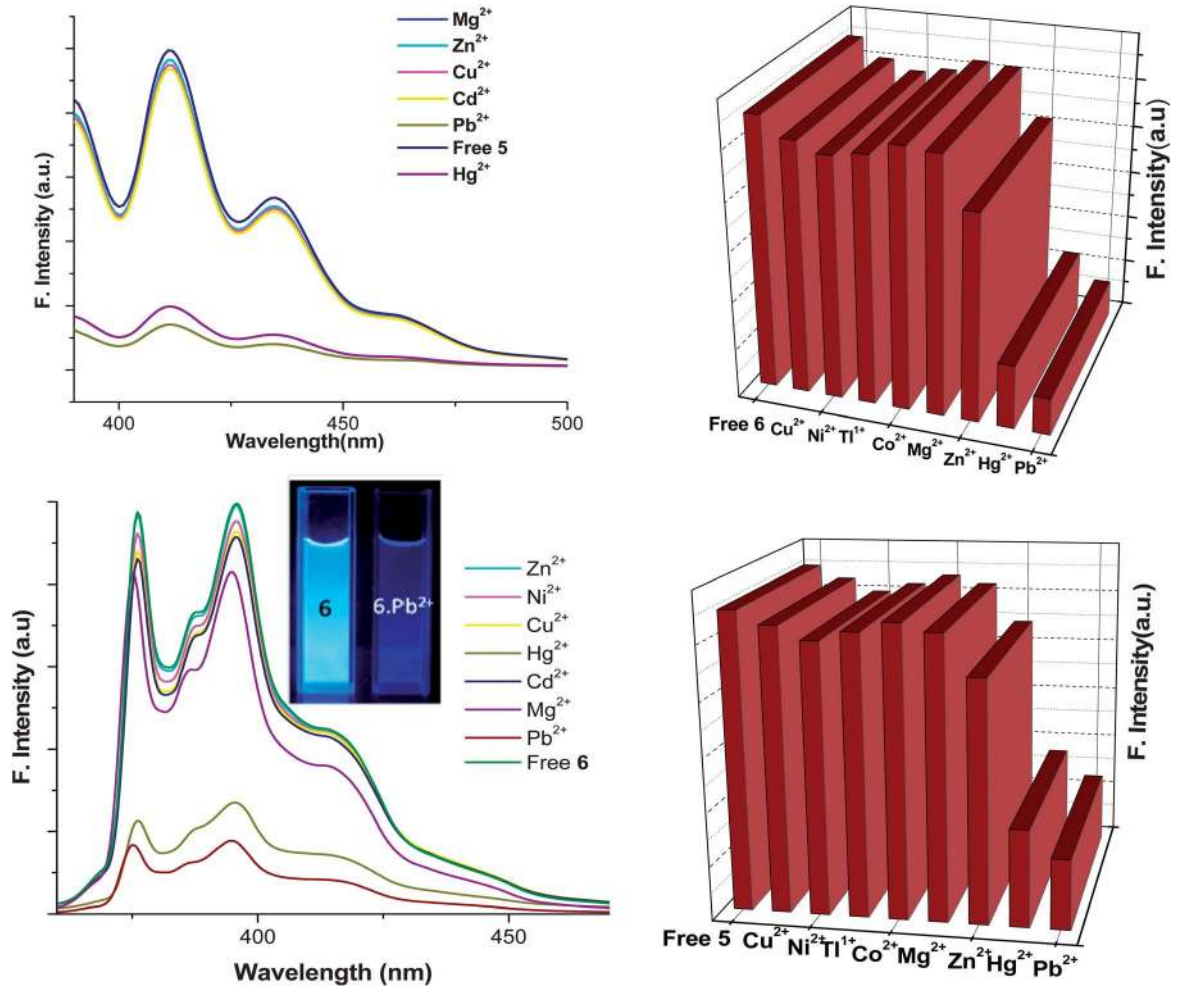

Fig. 5 Changes in the fluorescence spectra of **5** (top) and **6** (bottom) (1.5×10^{-10} M) upon addition of several cations. Bar plot representation of the fluorescence emission intensity of **5** (top) and **6** (bottom) upon the addition of several cations in aqueous media.

was treated separately with 0.5 equiv. of Cu^{2+} in presence of 0.5 equiv. each of interference metal ions (Pb^{2+}, Zn^{2+}, Cd^{2+}, Hg^{2+}, Mg^{2+}, Tl^{+} and Ca^{2+}). As shown in Fig. 7, small or no obvious interference with the detection of Cu^{2+} could be observed. These results evidently demonstrate the high selectivity for Cu^{2+} over other metal ions. In a similar fashion, a solution of **5** or **6** (1.5×10^{-10} M) was treated separately with 0.5 equiv. of Pb^{2+} in the presence of 0.5 equiv. each of interference metal ions (Cu^{2+}, Zn^{2+}, Cd^{2+}, Hg^{2+}, Mg^{2+}, Tl^{+} and Ca^{2+}) and the resulting titration shows (Fig. 7) no noticeable interference with the detection of Pb^{2+} except for Hg^{2+} ion.

Visual recognition of Hg^{2+} and Cu^{2+} ion

When an excess of different metal ions (Li^{+}, Na^{+}, K^{+}, Ca^{2+}, Ag^{+}, Mg^{2+}, Cr^{2+}, Zn^{2+}, Ni^{2+}, Co^{2+}, Cu^{2+}, Fe^{2+}, Tl^{+}, Cd^{2+}, Hg^{2+} and Pb^{2+}) were separately added to a solution of **3** and **4** in CH_3CN/H_2O, 2/8 (10^{-5} M), no significant color change was observed, except for Cu^{2+} which shows a radical colour change form light yellow to brown. In contrast, as shown in Fig. 8, upon addition of excess of different metal ions to the CH_3CN solution of **5** or **6**, only Pb^{2+} and Hg^{2+} ion shows drastic color change.

Reversibility interaction of 3 and [3·Cu^{2+}], 4 and [4·Cu^{2+}], 5 and [5·Hg^{2+}] and 6 and [6·Hg^{2+}]

The reversible interaction between **5** or **6** with Hg^{2+} was confirmed by the introduction of I^{-} into the system containing **5** or **6** (10^{-6} M) and Hg^{2+} ion. The experiment, shown in Fig. 9, showed that the addition of 2 equiv. of I^{-} into **5**·Hg^{2+} or **6**·Hg^{2+} immediately enhanced the fluorescence of **5** or **6**. When Hg^{2+} was further added to the system, the fluorescence of **5** or **6** was quenched again. This process could be repeated several times without loss of sensitivity of the fluorescence, which clearly demonstrates the high degree of reversibility of the complexation/decomplexation process between **5** or **6** and Hg^{2+} ions. The reversibility of the complexation process of **5** or **6** with Pb^{2+} ions was also tested by the same experiment as performed for Hg^{2+} ion and that also shows high level of reversibility of the complexation/decomplexation process. Similarly the reversible interactions of **3** and **4** with Cu^{2+} were studied with the chelating agent EDTA. It was also confirmed that the response of **3** or **4** to Cu(II) was reversible rather than a cation-catalyzed reaction[67,68] by the following experiments: (i) the color and fluorescence of **3**–Cu(II) disappeared instantly

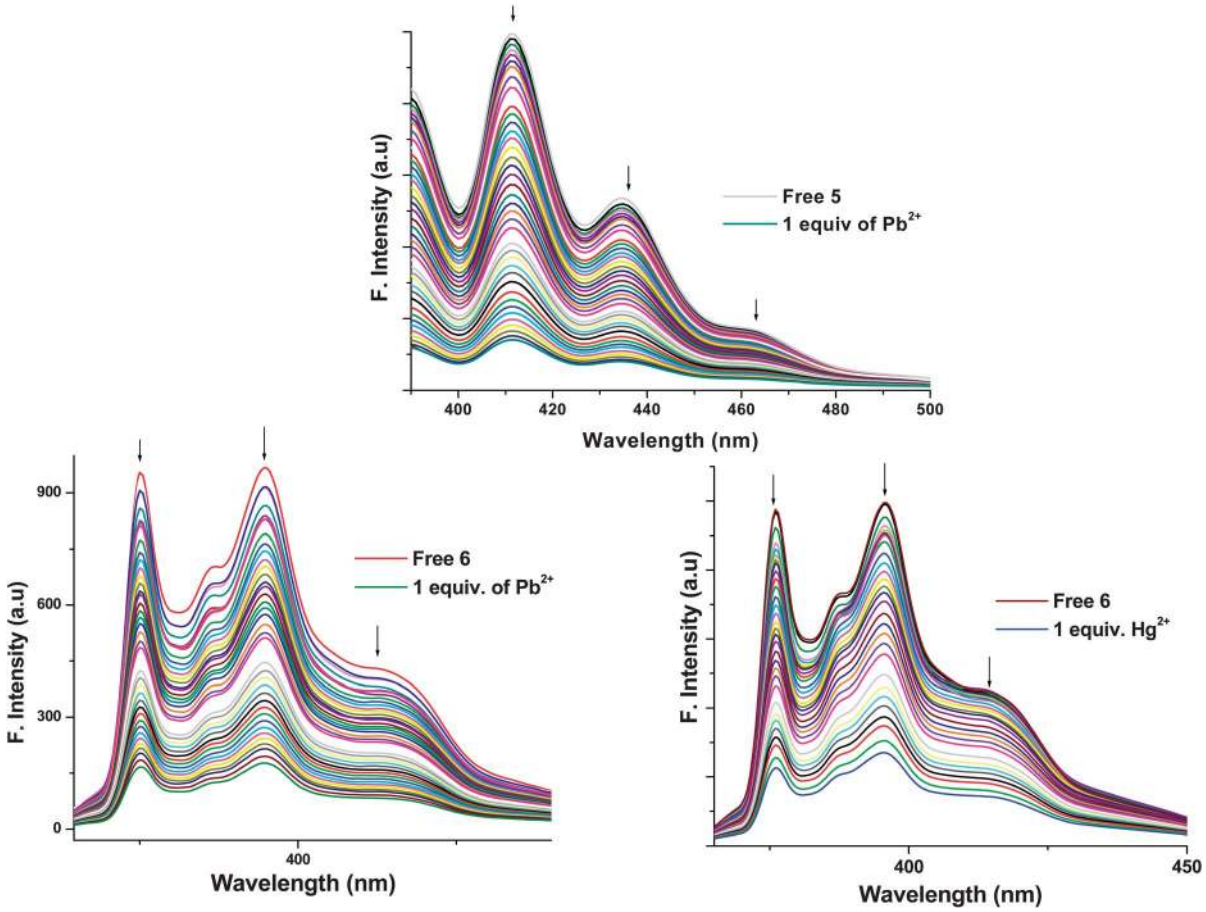

Fig. 6 Fluorescence emission changes of **5** (1.5×10^{-10} M) upon addition of Pb^{2+} ion (top) and **6** (bottom) (1.5×10^{-10} M) upon addition of Pb^{2+} ion (left) and Hg^{2+} ion (right) up to 1 equiv.

upon the addition of EDTA, whereas excess Cu(II) would recover the colour again; (ii) the TLC results and the mass spectra data of a solution containing 10 μM **3** or **4** and 12 μM Cu(II) after standing at room temperature for 2 days indicated no other chemical species except for **3** and **3**–Cu(II) or **4** and **4**–Cu(II).

To support the results obtained by spectrophotochemical experiments and to obtain additional information about the coordination mode of these metal cations by receptors **3–6**, we performed a ^{1}H NMR analysis for Cu^{2+} ion in CD_3CN solution. As shown in the Fig. 10 (left), the most significant ^{1}H NMR spectral changes observed upon the addition of increasing amounts of Cu^{2+} to a solution of the free receptor **4** are the following: (i) the hydrogen atom within the triazole ring significantly shifted by 0.23 ppm which indicates the coordination of Cu^{2+} ion with nitrogen atom of the amine group and (ii) the Ha atom shifted by 0.11 ppm which indicating the coordination of Cu^{2+} ion with oxygen atom as well, (iii) amine (NH) proton did not show any marked shift indicating no interaction with Cu^{2+} atom. Similarly, as shown in the Fig. 10 (right), the most significant ^{1}H NMR spectral changes observed upon the addition of increasing amounts of Pb^{2+} to a solution of the free receptor **6** are the (i) the hydrogen atom within the triazole ring significantly shifted by 0.27 ppm, (ii) Hb and Hc atom shifted by 0.18 and 0.12 ppm respectively. From the magnitude of the observed ^{1}H chemical shifts, it can be concluded that the plausible binding mode of Cu^{2+} is the oxygen atom of amide group and N atom of the triazole ring and for Pb^{2+} or Hg^{2+} the binding sites are the oxygen atom of OCH_2 group and N atom of the triazole ring (Fig. 11).

Based on ligand/cation binding ratio (Job's plot), ESI-MS data and ^{1}H NMR titration of receptors **3** and **4** with Cu^{2+}, we are able to provide the tentative binding mode of these receptors. We speculate that the high selectivity of **3** (or **4**) for Cu^{2+} is due to presence of amide group which create negative charge on O atom of CO group *via* electron transfer from NH moiety. In case of **5** and **6** Job's plot and ESI-MS data suggest that one ligand binds with one Pb^{2+} or Hg^{2+} ion. The selectivity of these receptors arise may be due to the complementary charge and size factor between the receptive site of the host and the guest ion. Further these tentative coordination modes of the receptors **3–6** were supported by DFT based quantum chemical calculations.

Theoretical calculations

The 1 : 1 ligand-to-metal complexation behavior of the receptors **3–6** determined by both mass spectrum and Job

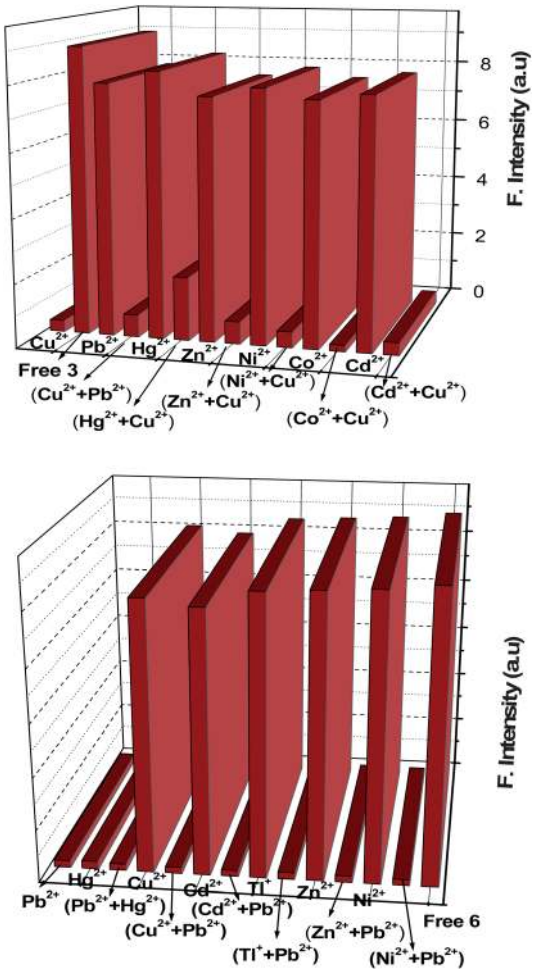

Fig. 7 Bar plot representation of changes in the fluorescence spectra of **3** (top) and **6** (bottom) (1.5×10^{-10} M) in CH_3CN/H_2O (2 : 8) upon addition of the several metal cations tested.

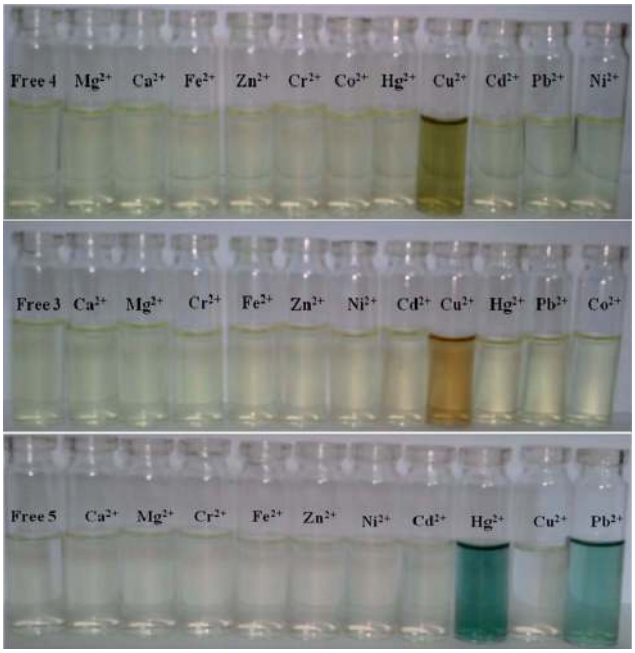

Fig. 8 Visual features observed of **3**–**5** (10^{-5} M) in CH_3CN/H_2O, (2/8) solution after addition of 5 equiv. of several cations tested.

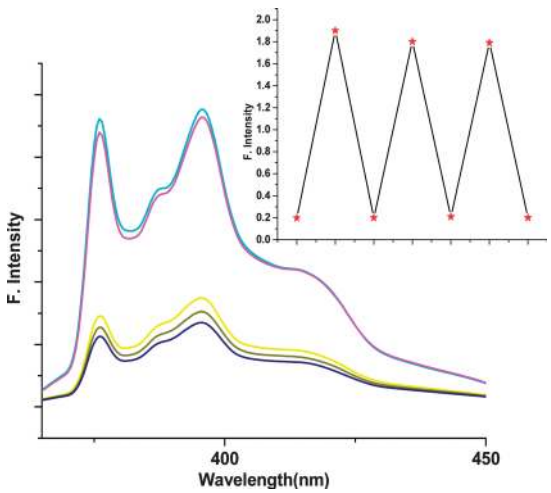

Fig. 9 Reversibility of the interaction between **6** and Hg^{2+} by the introduction of I^- to the system. Inset: stepwise complexation/decomplexation cycles carried out in CH_3CN/H_2O, (2/8) with **6** and Hg^{2+}.

plot measurements, was further supported by DFT. The receptors **3**–**6** with and without metal cation (Cu^{2+}, Pb^{2+} or Hg^{2+} ion) were subjected to the energy optimization at the Cam-B3LYP hybrid functional with 6–31G* basis set.[69] Several different starting geometries were used for the geometry optimization to ensure that the optimized structures corresponded to global minima. The optimized geometry for the ligands **3** and **5** is represented Fig. 12 and 13 respectively and the ligands **4** and **6** are shown in S19 (see ESI†) and the energy minimized structures for the ligands **3** and **5** and their corresponding complexes with metal ions are shown in Fig. 12 and 13. Binding of the divalent cations, has also been investigated by quantum chemical calculations. The structures for all the eight $[\mathbf{L}\cdot\mathrm{M}]^{2+}$ complexes (M = Hg, Pb, Cu; **L** = **3**, **4**, **5**) were calculated (as di-perchlorate species), which resulted to be quite similar to each other. In the complex $[\mathbf{L}\cdot\mathrm{Cu}](ClO_4)_2$ (**L** = **3** and **4** (SI, Fig. S18†)] Cu^{2+} centre lies in a square–pyramidal environment in such a way that all the donor atoms are arranged approximately perpendicular to each other. Both close Cu–N and Cu–O contacts (d_{Cu-N} = 2.05 Å and d_{Cu-O} = 1.974 Å) are typical for strong equatorial bonds, as evidenced by the relatively high values of Wiberg's bond index (WBI_{Cu-N} = 0.2596 and WBI_{Cu-O} = 0.2674) (SI, Table S1†). Three O atoms belonging to two perchlorate ligands occupy the other two equatorial (d_{Cu-O} = 2.009 and 1.951 Å; WBI_{Cu-O} = 0.2774 and 0.3183 respectively) and one weak axial (d_{Cu-O} = 2.296; WBI_{Cu-O} = 0.1738) positions around the Cu^{2+} cation. Whereas in the complex $\mathbf{L}\cdot\mathrm{M}](ClO_4)_2$ (**L** = **5** and **6**; M = Hg and Pb) the metal ion (both Hg^{2+} and Pb^{2+}) can be realized to occupy the octahedral position (Fig. 13, S20 and S21†).

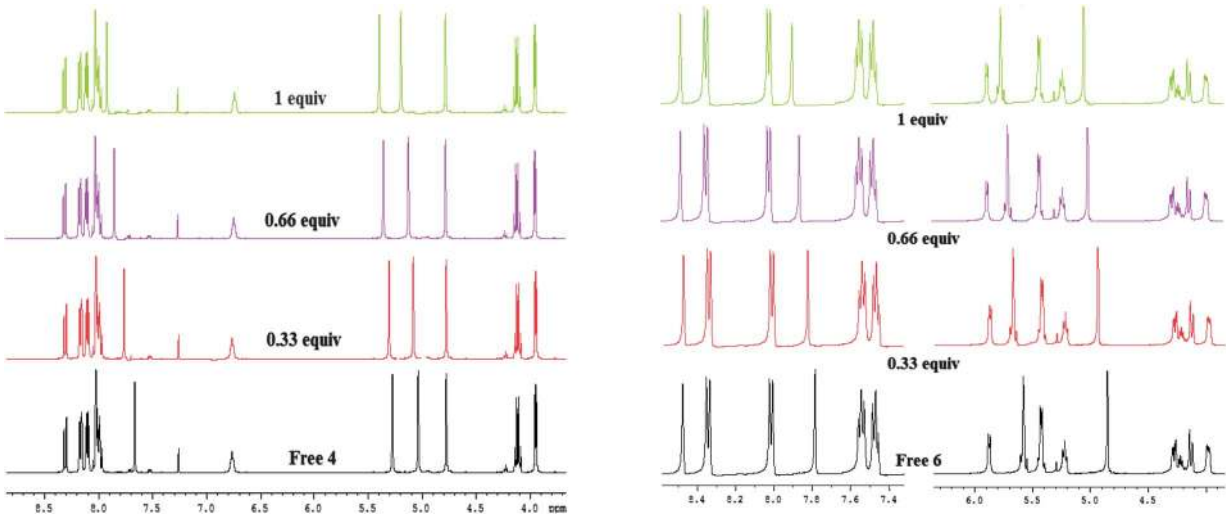

Fig. 10 ^{1}H NMR titration of **4** (left) upon addition of increasing amount of Cu^{2+} up to 1 equiv. and of **6** (right) upon addition of increasing amount of Pb^{2+} up to 1 equiv. in CD_3CN solution.

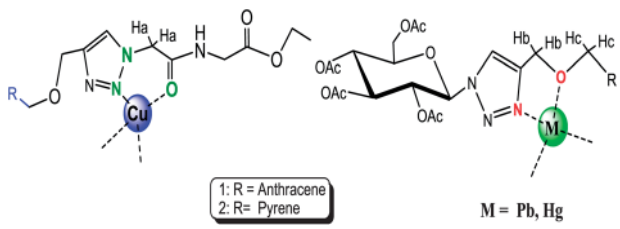

Fig. 11 The plausible binding modes for **3** and **4** (left) with Cu^{2+} ion and for **5** and **6** (right) with Pb^{2+}/Hg^{2+} ion.

Experimental

Materials and methods

The perchlorate salts of Li^{+}, Na^{+}, Tl^{+}, K^{+}, Ag^{+}, Ca^{2+}, Mg^{2+}, Cr^{2+}, Mn^{2+}, Fe^{2+}, Co^{2+}, Cu^{2+}, Zn^{2+}, Cd^{2+}, Ni^{2+}, Pb^{2+}, and Hg^{2+} were purchased from Aldrich and were directly used without further purification. Anthracene-9-carboxaldehyde, 1-pyrenecarboxaldehyde, (α)-D-glucose, ethyl ester-glycine hydrochloride, NaH, propargyl bromide, sodium ascorbate, glycine ethyl ester hydrochloride, sodium azide, acetonitrile (HPLC) were purchased from Aldrich and were used without further purification. Chromatography was carried out on 3 cm of silica gel in a column of 2.5 cm diameter. The column chromatography was carried out using 100–200 mesh silica gel. All the solvents were dried by conventional methods and distilled under Ar atmosphere before use. The UV-vis spectra were carried out in CH_3CN/H_2O solutions at $c = 1 \times 10^{-5}$ M as it is stated in the corresponding figure captions and the fluorescence spectra were carried out at $c \approx 10^{-10}$ M, as it is stated in the corresponding figure captions.

Instrumentation

The ^{1}H, ^{13}C NMR spectra were recorded on Bruker 400 MHz FT-NMR spectrometers, using tetramethylsilane as the internal reference. Electrospray ionization mass spectrometry (ESI-MS) measurements were carried out on a Qtof Micro YA263 HRMS instrument. The absorption spectra were recorded with a JASCO

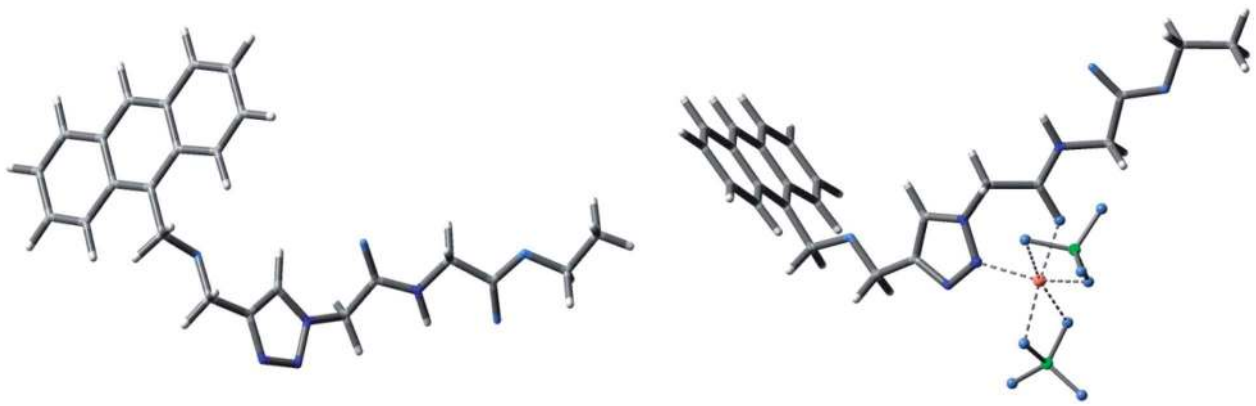

Fig. 12 Optimized geometry of **3** (left) and [**3**·Cu^{2+}] (right).

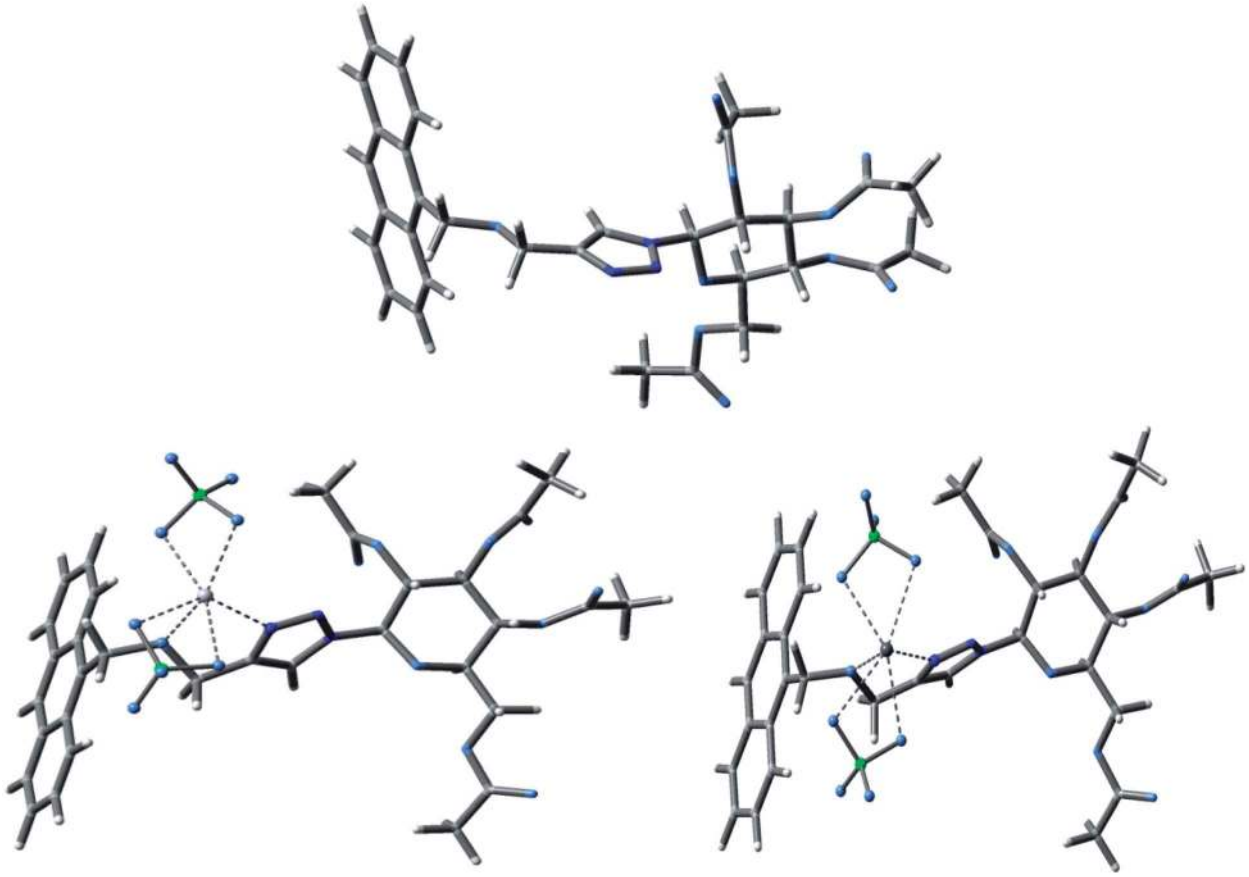

Fig. 13 Optimized geometry of **5** (top) and [**5**·Hg^{2+}] (below left) and [**5**·Pb^{2+}] (right).

V-650 UV-vis spectrophotometer at 298 K. Fluorescence was recorded with JASCO-FP-6300 spectrofluorometer.

Caution! metal pechlorate salts are potentially explosive in certain conditions. All due precautions should be taken while handling perchlorate salts!

Synthesis of 3 and 4

To a well-stirred solution of anthracene alkyne (0.5 g, 2.03 mmol) and glycine azide (0.37 g, 2.03 mmol) in 15 mL of acetone/H_2O (2 : 1) an aqueous solution of $CuSO_4 \cdot 5H_2O$ (0.101 g, 0.40 mmol) was added. A freshly prepared sodium ascorbate solution (0.160 g, 0.81 mmol) was added to this mixture and the resulting solution was stirred at room temperature for 12 h. A total of 30 mL of ethyl acetate was added to the reaction mixture, and the organic layer was washed several times with water and finally with brine (15 mL) and dried over anhydrous sodium sulfate. The solvent was removed under reduced pressure, and the crude product was purified by silica gel column chromatography. Elution with EtOAc/hexane (8 : 2, v/v) yielded light yellow **3** (0.60 g, 83%).

Compound **4** was synthesized using the same procedure above with the following chemicals: pyrene alkyne (0.5 g, 3.33 mmol), glycine azide (0.62 g, 3.33 mmol), $CuSO_4 \cdot 5H_2O$ (0.166 g, 0.66 mmol), sodium ascorbate solution (0.264 g, 1.33 mmol) and it yielded light yellow **4** (0.64 g, 84%).

3: ^{1}H NMR ($CDCl_3$, 400 MHz): δ = 8.39 (s, 1H, $H_{anthracene}$), 8.29–8.27 (m, 2H, $H_{anthracene}$), 7.95–7.93 (m, 2H, $H_{anthracene}$), 7.55–7.41 (m, 4H, $H_{anthracene}$), 7.40 (s, 1H, $H_{triazole}$), 7.15(s, 1H, NH_{proton}), 5.49 (s, 2H, CH_2–$N_{triazole}$), 4.92 (s, 2H, $OCH_{2anthracene}$), 4.76 (s, 2H, OCH_2–triazole), 4.1–4.01(q, 2H, OCH_{2ester}), 4.38 (s, 2H, CH_{2ester}), 1.17–1.14 (t, 3H, CH_{3ester}); ^{13}C NMR ($CDCl_3$, 100 MHz): δ = 169.2, 165.6, 145.5, 131.3, 130.9, 129.0, 128.6, 126.4, 125.0, 124.6, 124.2, 64.6, 63.7, 61.5, 60.4, 52.4; electrospray MS, *m*/*z* (relative intensity): 433 (M^+ + 1), anal. calcd for $C_{24}H_{24}O_4N_4$ C, 66.64; H, 5.60; N, 12.96. Found: C, 66.37; H, 5.38; N, 12.58%.

4: ^{1}H NMR ($CDCl_3$, 400 MHz): δ = 8.29 (s, 1H, H_{pyrene}), 8.17–7.98 (m, 8H, H_{pyrene}), 7.66 (s, 1H, $H_{triazole}$), 6.76 (s, 1H, NH_{proton}), 5.27 (s, 2H, CH_2–$N_{triazole}$), 5.03 (s, 2H, $OCH_{2pyrene}$), 4.77 (s, 2H, OCH_2–triazole), 4.1–4.08 (q, 2H, OCH_{2ester}), 3.9 (d, 2H, CH_{2ester}), 1.2–1.1 (t, 3H, CH_{3ester}); ^{13}C NMR ($CDCl_3$, 100 MHz): δ = 169.0, 165.3, 145.8, 131.4, 131.2, 130.7, 129.4, 127.8, 127.5, 127.3, 127.2, 125.9, 125.2, 124.8, 124.6, 124.5, 124.3, 123.3, 71.1, 63.5, 61.6, 52.6, 41.38; electrospray MS, *m*/*z* (relative intensity): 457 (M^+ + 1); anal. calcd for $C_{26}H_{24}O_4N_4$ C, 68.39; H, 5.30; N, 12.28. Found: C, 68.67; H, 5.55; N, 12.15%.

Synthesis of compounds 5 and 6

Compounds **5** and **6** were prepared in good yield following the procedure adopted for **3** and the following chemicals are used. **5**: anthracene alkyne (0.5 g, 2.03 mmol), (α)-D-glucose azide (0.78 g, 2.03 mmol), aqueous $CuSO_4 \cdot 5H_2O$ (0.101 g, 0.40 mmol), and

sodium ascorbate (0.160 g, 0.81 mmol); **6**: pyrene alkyne (0.5 g, 3.33 mmol), (α)-D-glucose azide (1.28 g, 3.33 mmol), aqueous $CuSO_4 \cdot 5H_2O$ (0.166 g, 0.66 mmol), sodium ascorbate (0.264 g, 1.33 mmol). The crude product was purified by silica gel column chromatography and elution with EtOAc/hexane (7 : 2, v/v) to yield pure light yellow **5** (0.73 g, 85%), **6** (0.91 g, 85.05%).

5: ^{1}H NMR ($CDCl_3$, 400 MHz): δ = 8.39 (s, 1H, $H_{anthracene}$), 8.29–8.27 (m, 2H, $H_{anthracene}$), 7.95–7.93 (m, 2H, $H_{anthracene}$), 7.55–7.41 (m, 4H, $H_{anthracene}$), 7.40 (s, 1H, $H_{triazole}$), 4.81 (s, 2H, OCH_2–acetate), 5.29 (s, 1H), 4.28–4.24 (m, 1H), 4.13–4.10 (m, 1H), 3.99–3.95 (m, 1H), 2.06–2.03 (m, 9H, $CH_{3acetate}$), 1.876 (s, 3H, $CH_3OCH_{2acetate}$); ^{13}C NMR ($CDCl_3$, 100 MHz): δ = 145.3, 134.2, 131.4, 131.0, 129.0, 128.6, 126.3, 125.0, 124.3, 122.0, 80.8, 69.2, 68.9, 64.6, 64.1, 50.1; electrospray MS, *m*/*z* (relative intensity): 620 (M^+ + 1); anal. calcd for $C_{32}H_{33}O_{10}N_3$ C, 62.01; H, 5.37; N, 6.78. Found: C, 62.08; H, 5.18; N, 7.43%.

6: ^{1}H NMR ($CDCl_3$, 400 MHz): δ = 8.36 (s, 1H, H_{pyrene}), 8.35–7.99 (m, 8H, H_{pyrene}), 7.80 (s, 1H, $H_{triazole}$), 5.88 (s, 1H, H), 5.42 (s, 2H, OC$H_{2pyrene}$), 5.41 (s, 2H, OCH_2–triazole), 4.81 (s, 2H, OCH_2–acetate), 5.29 (s, 1H), 4.28–4.24 (m, 1H), 4.13–4.10 (m, 1H), 3.99–3.95 (m, 1H), 2.06–2.03 (m, 9H, $CH_{3acetate}$), 1.876 (s, 3H, $CH_3OCH_{2acetate}$); ^{13}C NMR ($CDCl_3$, 100 MHz): δ = 170.5, 169.9, 169.3, 168.9, 146.0, 131.4, 131.2, 130.8, 130.7, 129.4, 127.8, 127.5, 127.2, 125.9, 20.68; electrospray MS, *m*/*z* (relative intensity): 644 (M^+ + 1); anal. calcd for $C_{34}H_{33}O_{10}N_3$ C, 63.43; H, 5.17; N, 6.53. Found: C, 63.37; H, 5.08; N, 7.03%.

Conclusions

In closing, we have successfully developed triazole-based, easy-to synthesize fluorescent chemosensors **3**–**6** and examined their binding properties towards various guest cations through optical and spectral techniques, as well as by DFT-based quantum chemical calculations. Interestingly, upon fine tuning of the sensory unit from amino acid to carbohydrate the selectivity of the receptors was found to change from Cu(II) to Pb(II)/Hg(II). The binding of Cu^{2+} ions with receptors **3** and **4** is ultrasensitive and highly selective allowing selective detection in the presence of competitive non-transition and transition-metal ions alike. The receptors, based on a small molecule that can selectively detect Cu^{2+} ions at the 0.89 ppb level in aqueous environments, are unprecedented. Both receptors **5** and **6** show an excellent selectivity and sensitivity towards Hg^{2+} and Pb^{2+} ion in aqueous environments. Although the carbohydrate-based metal ion sensor molecules are scarce in the literature, **5** and **6** are unique molecular systems that work well in detecting very low concentrations of Pb^{2+} or Hg^{2+}, even in the presence of a wide range of competitive cations. Furthermore, these receptors, **5** and **6** are capable of detecting Hg^{2+}/Pb^{2+} ions in river water samples. Therefore, we believe that all the receptors described in this article may be used for many practical applications in chemical and biological systems.

Acknowledgements

Generous support of the Department of Science and Technology, DST, (Grant no. SR/S1/IC-13/2011), New Delhi is gratefully acknowledged. A.T. thanks Council of Scientific and Industrial Research (CSIR) India for senior research fellowships.

Notes and references

1 A. P. de Silva, H. Q. N. Gunaratne, T. Gunnlaugsson, J. M. A. Huxley, C. P. Mc Coy, J. T. Rademacher and T. E. Rice, *Chem. Rev.*, 1997, **97**, 1515.
2 B. Valeur and I. Leray, *Coord. Chem. Rev.*, 2000, **205**, 33.
3 K. Rurack, *Spectrochim. Acta.*, 2001, **57A**, 2161.
4 V. Amendola, L. Fabbrizzi, F. Forti, M. C. Mangano, P. Pallavicini, A. D. Poggi and A. Taglieti, *Coord. Chem. Rev.*, 2006, **250**, 273.
5 C. J. Chang, E. M. Nolan, J. Jaworski, S. C. Burdette, M. Sheng and S. J. Lippard, *Chem. Biol.*, 2004, **11**, 203.
6 E. M. Nolan, S. C. Burdette, J. H. Harvey, S. A. Hilderbrand and S. J. Lippard, *Inorg. Chem.*, 2004, **43**, 2624.
7 C. J. Chang, E. M. Nolan, J. Jaworski, K.-I. Okamoto, Y. Hayashi, M. Sheng and S. J. Lippard, *Inorg. Chem.*, 2004, **43**, 6774.
8 E. M. Nolan and S. J. Lippard, *Inorg. Chem.*, 2004, **43**, 8310.
9 N. C. Lim and C. Brückner, *Chem. Commun.*, 2004, 1094.
10 K. Komtsu, K. Kakuchi, H. Kojima, Y. Urano and T. Nagono, *J. Am. Chem. Soc.*, 2005, **127**, 10197.
11 C. C. Woodroofe, A. C. Won and S. J. Lippard, *Inorg. Chem.*, 2005, **44**, 3112.
12 M. Taki, J. L. Wolford and T. V. O'Halloran, *J. Am. Chem. Soc.*, 2004, **126**, 712.
13 N. C. Lim, J. V. Schuster, M. C. Porto, M. A. Tanudra, L. Yao, H. C. Freake and C. Brückner, *Inorg. Chem.*, 2005, **44**, 2018.
14 X.-M. Meng, M.-Z. Zhu, L. Liu and Q.-X. Guo, *Tetrahedron Lett.*, 2006, **47**, 1559.
15 Z. Xu, X. Qian, J. Cui and R. Zhang, *Tetrahedron Lett.*, 2006, **62**, 10117.
16 S. Aoki, K. Sakurama, N. Matsuo, Y. Yamada, R. Takasawa, S.-i. Tanuma, M. Shiro, K. Takeda and E. Kimura, *Chem.–Eur. J.*, 2006, **12**, 9066.
17 X.-L. Ni, S. Wang, X. Zeng, Z. Tao and T. Yamato, *Org. Lett.*, 2010, **13**, 552.
18 A. Renzoni, F. Zino and E. Franchi, *Environ. Res., Sect. A*, 1998, **77**, 68.
19 P. B. Tchounwou, W. K. Ayensu, N. Ninashvili and D. Sutton, *Environ Toxicol Chem*, 2003, **18**, 149.
20 J. S. Lin-Fu, *Lead Poisoning, A Century of Discovery and Rediscovery, in Human Lead Exposure*, ed. H. L. Needleman, Lewis Publishing, Boca Raton, FL, 1992.
21 G. Muthaup, A. Schlicksupp, L. Hess, D. Beher, T. Ruppert, C. L. Masters and K. Beyreuther, *Science*, 1996, **271**, 1406.
22 R. A. Løvstad, *BioMetals*, 2004, **17**, 111.
23 K. J. Barnham, C. L. Masters and A. I. Bush, *Nat. Rev. Drug Discovery*, 2004, **3**, 205.
24 D. R. Brown and H. Kozlowski, *Dalton Trans.*, 2004, 1907.
25 G. L. Millhauser, *Acc. Chem. Res.*, 2004, **37**, 79.
26 E. Gaggelli, H. Kozlowski, D. Valensin and G. Valensin, *Chem. Rev.*, 2006, **106**, 1995.

27 S. Saha, P. Mahato, M. Baidya, S. K. Ghosh and A. Das, *Chem. Commun.*, 2012, 9293.
28 P. Mahato, S. Saha, E. Suresh, R. Di Liddo, P. P. Parnigotto, M. T. Conconi, M. K. Kesharwani, B. Ganguly and A. Das, *Inorg. Chem.*, 2012, **51**, 1769.
29 S. Saha, M. U. Chhatbar, P. Mahato, L. Praveen, A. K. Siddhanta and A. Das, *Chem. Commun.*, 2012, 1659.
30 S. Saha, P. Mahato, U. G. Reddy, E. Suresh, A. Chakrabarty, M. Baidya, S. K. Ghosh and A. Das, *Inorg. Chem.*, 2012, **51**, 336.
31 P. Mahato, A. Ghosh, S. Saha, S. Mishra, S. K. Mishra and A. Das, *Inorg. Chem.*, 2010, **49**, 11485.
32 A. K. Mandal, M. Suresh, P. Das, E. Suresh, M. Baidya, S. K. Ghosh and A. Das, *Org. Lett.*, 2012, **14**, 2980.
33 M. Suresh, A. Ghosh and A. Das, *Chem. Commun.*, 2008, 3906.
34 J. Zhang, B. Li, L. Zhang and H. Jiang, *Chem. Commun.*, 2012, 4860.
35 M.-Q. Wang, K. Li, J.-T. Hou, M.-Y. Wu, Z. Huang and X.-Q. Yu, *J. Org. Chem.*, 2012, **77**, 8350.
36 J. Isaad and A. E. Achariab, *Dyes Pigm.*, 2013, **99**, 878.
37 J. Isaad and A. E. Achariab, *Analyst*, 2013, **138**, 3809.
38 J. Isaad and A. E. Achariab, *Tetrahedron*, 2013, **69**, 4866.
39 F. Otón, M. del C. González, A. Espinosa, A. Tárraga and P. Molina, *Organometallics*, 2012, **31**, 2085.
40 F. Otón, M. del C. González, A. Espinosa, C. Ramírez de Arellano, A. Tárraga and P. Molina, *J. Org. Chem.*, 2012, **77**, 10083.
41 V. Ganesh, V. S. Sudhir, T. Kundu and S. Chandrasekaran, *Chem.–Asian J.*, 2011, **6**, 2670.
42 E. Ermakova, J. Michalak, M. Meyer, V. Arslanov, A. Tsivadze, R. Guilard and A. B. -Lemeune, *Org. Lett.*, 2013, **15**, 662.
43 A. Caballero, R. Martinez, V. Lloveras, I. Ratera, J. Vidal-Gancedo, K. Wurst, A. Tarraga, P. Molina and J. Veciana, *J. Am. Chem. Soc.*, 2005, **127**, 15666.
44 A. Thakur and S. Ghosh, *Organometallics*, 2012, **31**, 819.
45 A. Thakur, S. Sarder and S. Ghosh, *Inorg. Chem.*, 2011, **50**, 7066.
46 A. Thakur, S. Sardar and S. Ghosh, *J. Chem. Sci.*, 2012, **124**, 1255.
47 A. Thakur, D. Mandal and S. Ghosh, *Anal. Chem.*, 2012, **85**, 1665.
48 A. Thakur, D. Mandal and S. Ghosh, *J. Organomet. Chem.*, 2013, **726**, 71.
49 D. Mandal, P. Deb, B. Mondal, A. Thakur, J. Pooniah and S. Ghosh, *RSC Adv.*, 2013, **3**, 18614.
50 J. Huang, Y. Xu and X. Qian, *J. Organomet. Chem.*, 2009, **74**, 2167.
51 H. Lu, L. Xiong, H. Liu, M. Yu, Z. Shen, F. Li and X. You, *Org. Biomol. Chem.*, 2009, **7**, 2554.
52 J. Gong, T. Zhou, D. Song, L. Zhang and X. Hu, *Anal. Chem.*, 2010, **82**, 567.
53 F. Loe-Mie, G. Marchand, J. Berthier, N. Sarrut, M. Pucheault, M. Blanchard-Desce, F. Vinet and M. Vaultier, *Angew. Chem., Int. Ed.*, 2010, **49**, 424.
54 A. Mallick and N. Chattopadhyay, *Photochem. Photobiol.*, 2005, **81**, 419.
55 K. A. Connors, *Binding Constants: The Measurement of Molecular Complex Stability*, Wiley-Interscience, New York, 1987.
56 D. S. McClure, *J. Chem. Phys.*, 1952, **20**, 682.
57 A. Varnes, W. R. B. Dodson and E. L. Wehry, *J. Am. Chem. Soc.*, 1972, **94**, 946.
58 M. Shortreed, R. Kopelman, M. Kuhn and B. Hoyland, *Anal. Chem.*, 1996, **68**, 1414.
59 http://www.epa.gov/safewater/contaminants/index.html, accessed June 2008.
60 D. Y. Wu, W. Huang, C. Y. Duan, Z. H. Lin and Q. J. Meng, *Inorg. Chem.*, 2007, **46**, 1538.
61 S. Yoon, A. E. Albers, A. P. Wong and C. J. Chnag, *J. Am. Chem. Soc.*, 2005, **127**, 16030.
62 W. Huang, P. Zhou, W. Yan, C. He, L. Xiong, F. Li and C. Duan, *J. Envior. Monit.*, 2009, **11**, 330.
63 N. M. Buie, V. S. Talanov, R. J. Butcher and G. G. Talanova, *Inorg. Chem.*, 2008, **47**, 3549.
64 Q. He, E. W. Miller, A. P. Wong and C. J. Chang, *J. Am. Chem. Soc.*, 2006, **128**, 9316.
65 H. A. Benesi and J. H. Hildebrand, *J. Am. Chem. Soc.*, 1949, **71**, 2703.
66 $1/\Delta I = 1/\Delta I_{max} + (1/K[C])(1/\Delta I_{max})$ ($\Delta I = I - I_{min}$ and $\Delta I_{max} = I_{max} - I_{min}$), where I, I_{min} and I_{max} are the emission intensities of **3–6** considered in an intermediate metal ion concentration, in the absence of metal ion and at a concentration of complete interaction, respectively, and K is the binding constant and [C] is the metal ion concentration. From the plot of $(I_{max} - I_{min})/(I - I_{min})$ against [C] − 1, the value of $K(\pm 15\%)$ extracted from the slope.
67 V. Dujols, F. Ford and A. W. Czarnik, *J. Am. Chem. Soc.*, 1997, **119**, 7386.
68 Y.-K. Yang, K.-J. Yook and J. Tae, *J. Am. Chem. Soc.*, 2005, **127**, 16760.
69 See the SI† for full computational details.

